2019

Seismic performance of reinforced concrete frames retrofitted using external superelastic shape memory alloy bars

Yamen Ibrahim Elbahy
The University of Western Ontario

Maged A. Youssef
Western University, youssef@uwo.ca

Mohamed E. Meshaly
Alexandria University

Seismic Performance of Reinforced Concrete Frames Retrofitted Using External Superelastic Shape Memory Alloys Bars

Y.I. Elbahy

Ph.D. Candidate, Department of Civil and Environmental Engineering,

The University of Western Ontario

London, Ontario, Canada, N6A 5B9

M.A. Youssef

Professor, Department of Civil and Environmental Engineering,

The University of Western Ontario

London, Ontario, Canada, N6A 5B9

M. Meshaly

Associate Professor, Structural Engineering Department,

Alexandria University

Alexandria, Egypt

Corresponding Author: **M.A. Youssef**

Email: youssef@uwo.ca,

Fax: 519-661-3779,

Phone: 519-661-2111, Ext: 88661

ABSTRACT

Pre-1970s designed and built reinforced concrete frame structures are considered unsafe when subjected to seismic loads. Insufficient anchorage of the beam reinforcement in the beam-column joints of these structures is considered a main deficiency. Newly built frame structures are seismically designed for safety, where high inelastic deformations can occur under moderate to strong earthquakes. Minimizing these inelastic deformations makes the structure repairable. One way to minimize these residual deformations is by using smart materials such as superelastic Shape Memory Alloys (SMAs). In this paper, the seismic performance of RC frames retrofitted using external superleastic SMA bars is investigated and compared to the behaviour of a regular steel RC frame structure. Nonlinear time history analysis is performed for a six storey RC frame structure located in a high seismic region. After performing the analysis, two retrofitted frames are assumed and analayzed at the load intensities causing failure of the steel RC frame. The performance of the retrofitted frames is compared to the steel RC frame in terms of the damage level, the Maximum Inter-Storey Drift (MID) ratio, Maximum Residual Inter-Storey Drift (MRID), Maximum Roof Drift Ratio (MRDR), Residual Roof Drift Ratio (RRDR), and the earthquake intensity at collapse. Analysis results show improved seismic performance for the two retrofitted frames as compared to the original steel RC frame. This improvement was represented by lower level of damage at the same earthquake intensity; small reduction (10% to 15%) in the MID and MRDR values; significant reduction (50%-70%) in the MRID and RRDR; and increased seismic capacity.

Keywords: reinforced concrete (RC); shape memory alloys (SMAs); moment frame; seismic damage; seismic residual deformations; and retrofitting.

1 INTRODUCTION

Reinforced Concrete (RC) frame structures designed and built prior to the 1970s lack ductility, and, thus, are unsafe under seismic loads (Hassan 2011). The beam-column joints (BCJs) of these structures are poorly detailed and are considered deficient under lateral loads. Beam reinforcement is insufficiently anchored into the joint area of these structures.

Newly built RC frame structures are designed to dissipate the energy of moderate and strong earthquakes through allowing some inelastic deformations (Engindeni 2008). These inelastic deformations result in permanent deformations in the structure, and in some cases may require demolishing the damaged structure. Thus, there is a need to retrofit the pre-1970s structures to be able to resist the seismic loads, and to reduce the permanent deformations of the newly built structures. One of the methods to achieve this goal is by utilizing smart materials such as superelastic Shape Memory Alloys (SMAs) (Alam et al. 2009; Youssef and Elfeki 2012).

Superleastic SMA bars have unique properties compared to the usual steel reinforcement. They can undergo large deformations and return to their undeformed shape upon unloading (Alam et al. 2007). They also have good resistance to fatigue and corrosion and high damping ability (Janke et al. 2005). So, using superleastic SMA bars to enhance the seismic performance of these structures can be ideal (Alam et al. 2009; Youssef and Elfeki 2012).

Youssef and Elfeki (2012) studied the behaviour of RC frame structures internally reinforced with SMA bars at the critical locations of the structure. Seven different arrangements for the SMA bars were selected resulting in seven different frames. Nonlinear dynamic analyses were performed to

select the frames with the best seismic performance. It was found that the frames with SMA reinforcement in the BCJs of the first floor, and in the BCJs of the first and fourth floors gave the best seismic performance.

This paper investigates the seismic performance of mid-rise RC frame structures retrofitted using external superleastic SMA bars. A six-storey steel RC frame located in a high seismic region is used as the reference frame. Two potential retrofit schemes, which utilize superelastic SMA bars, are assumed. Nonlinear dynamic analyses are performed for the three frames using Seismostruct software (Seismostruct 2018). Results of the analysis are then used to compare the seismic performance of the three frames in terms of the damage level, the Maximum Inter-Storey Drift (MID) ratio, Maximum Residual Inter-Storey Drift (MRID), Maximum Roof Drift Ratio (MRDR), Residual Roof Drift Ratio (RRDR), and the earthquake intensity at collapse. Enhanced performance is observed for the two retrofitted frames as compared to the original steel RC frame.

2 PROPOSED RETROFITTING TECHNIQUE

The idea of the proposed retrofitting technique is based on attaching external SMA bars to the RC BCJ. As shown in **Fig. 1**, the bars are attached to the BCJ using external steel angles. The steel angles are attached to the BCJ using steel bolts. One angle is attached to the BCJ joint area, while the second angle is attached to the beam. Hold down plates can be used for long SMA bars to force them to deform with the beam.

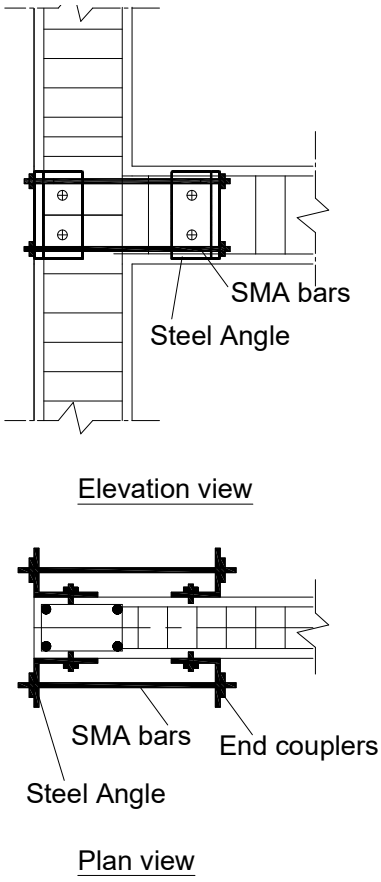

Fig. 1: Proposed retrofitting technique

The modulus of elasticity of SMA is much lower (1/5 to 1/3) than that of the regular steel. Thus, attaching a small to moderate ratio of SMA will improve the strength and the stiffness of the BCJ, but it is not expected to reduce the residual deformations at complete unloading. Thus, it is proposed to cut the internal steel bars of the beam at the face of the column and replace it with the external SMA bars. This ensures that the BCJ behaviour is governed by the external SMA bars rather than the internal steel bars, and, thus, minimum residual deformations are expected at complete unloading.

3 SIMPLIFIED MODEL

A simplified model for the retrofitted BCJ is proposed. The simplified model is developed using Seismostruct software v.6 (Seismostruct 2018). The special technique used to model the connection include: (i) modelling the SMA bars using inelastic truss elements; (ii) modelling the superelastic behaviour of the SMA bars using the uniaxial material model proposed by Auricchio and Sacco (1997); (iii) modelling the concrete beam and column using displacement based inelastic frame elements; and (iv) modelling the external angles that support the SMA bars using rigid arms connected to the concrete beam and column.

As shown in **Fig. 2**, the beam and the column of the BCJ are modelled using frame elements. Two rigid arms are connected to the beam near the face of the column to represent the angle that is bolted to the joint. Two additional rigid arms are connected to the beam at a distance equal to the length of the required SMA bars. The SMA bars connect the rigid arms and are modelled using truss elements. The reinforcement in the beam element is cut in between the rigid arms.

To validate the used modeling technique, the beam-column joint tested by Youssef et al. (2008) was utilized. The beam of the joint has a length of 1830 mm, 400 mm cross-section height, and 250 mm cross-section width, **Fig. 3**. Stirrups are 10M in diameter and are spaced at 80 mm for the 800 mm length, adjacent to the column, and spaced at 120 mm, elsewhere. The longitudinal top and bottom steel for the beam is 2-20M. Average concrete compressive strength of 53.50 MPa is used in the analysis. Steel reinforcing bars have yield strength of 450 MPa, ultimate strength 650 MPa, and a modulus of elasticity of 193 GPa. Stirrups have a yield strength of 422 MPa, and ultimate strength of 682 MPa. Used SMA bars have a critical stress equal to 401 MPa at a critical

strain of 0.75%. The modulus of elasticity is evaluated as 62.5 GPa. The residual strain is 0.73%, when the SMA bar was loaded up to 6.0% strain.

Predictions of the simplified model, developed using Seismostruct software, are compared to the predictions of a detailed Finite Element (FE) model developed using ABAQUS (ABAQUS 2018). The detailed FE model is developed using 8-node hexahedral isoparametric solid elements with reduced integration (C3D8R) and is shown in **Fig. 4**. These elements are used in the modelling process of the concrete, internal and external reinforcement, and external angles. Different element sizes are first considered to determine the appropriate mesh size. **Fig. 5** shows a comparison between the load-displacement results of both the simplified and detailed FE results. Good agreement in terms of initial stiffness, maximum strength, and residual displacement at complete unloading is achieved.

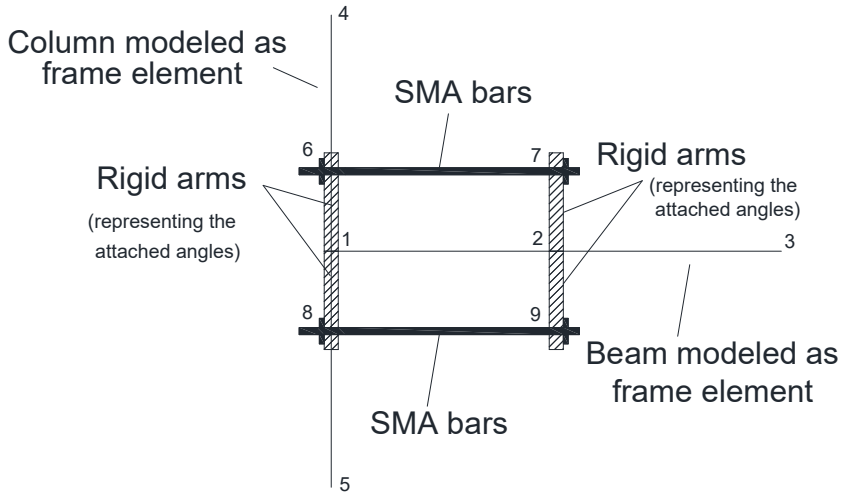

Fig. 2: Sketch of the simplified model

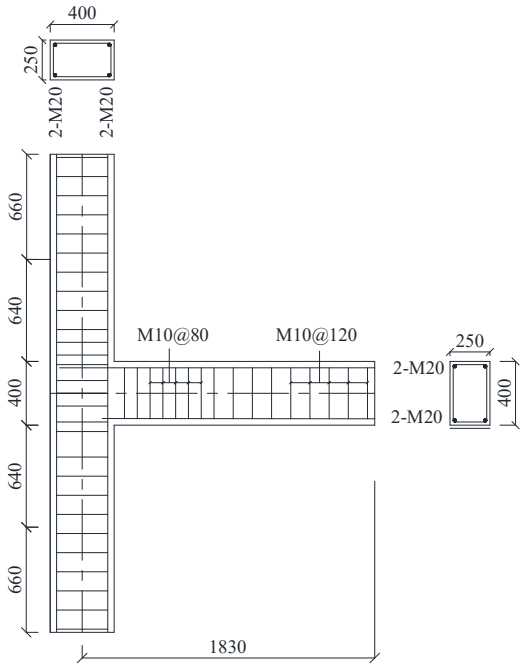

Fig. 3: Details of the BCJs tested by Youssef et al. (2008)

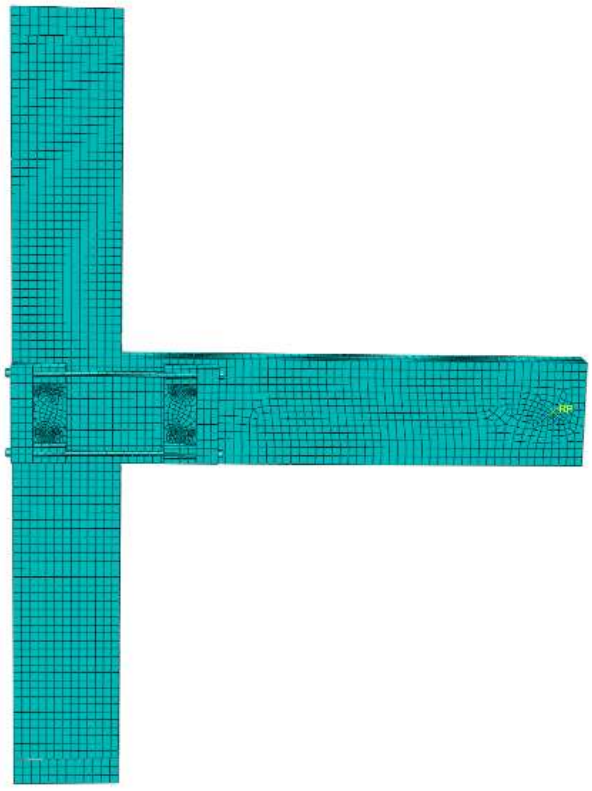

Fig. 4: FE Model of the retrofitted BCJ

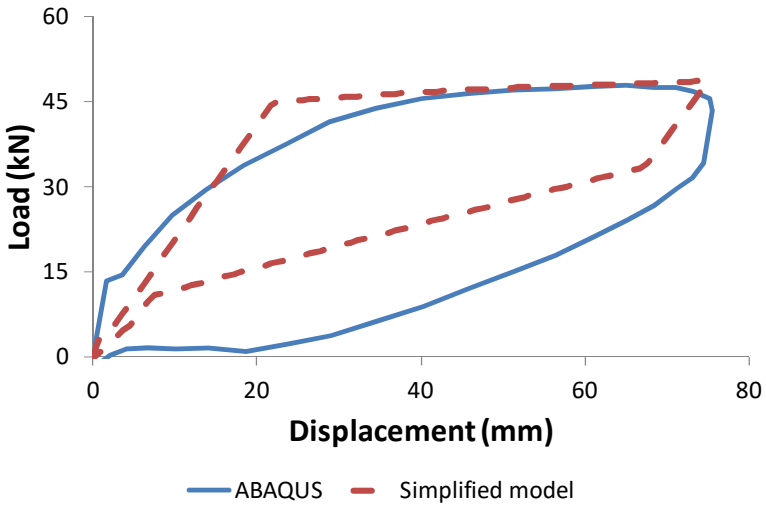

Fig. 5: Load-displacement results of the ABAQUS model vs. the simplified Seismostruct model

4 STEEL RC FRAME CHARACTERISTICS AND MODELING

The steel RC building, designed by Youssef and Elfeki (2012), is used as the reference frame. The building is a symmetric six-storey RC office building located in California (high seismic region). The layout and dimensions of the building are shown in **Fig. 6**. It is designed to satisfy the requirements of the International Building Code (IBC 2006) and the American Concrete Institute (ACI 318 2005). The lateral load resisting system is composed of special moment frames. The cross-section dimensions and the reinforcement details of the steel RC frame (Frame 1) are shown in **Fig. 7**.

Only one special moment frame is selected for the analysis because of the geometrical symmetry. The frame is modeled using Seismostruct software (Seismostruct 2018). The beams and columns are modeled using cubic elasto-plastic elements. The beams are divided in six elements, while the columns are divided in three. The beams are modeled as T-sections, while the beam-column joints

are modeled using rigid elements, **Fig. 8**. The length of the rigid element is 228.60 mm in each direction. The concrete compressive strength is assumed to be 28 MPa while the steel yielding stress is 400 MPa.

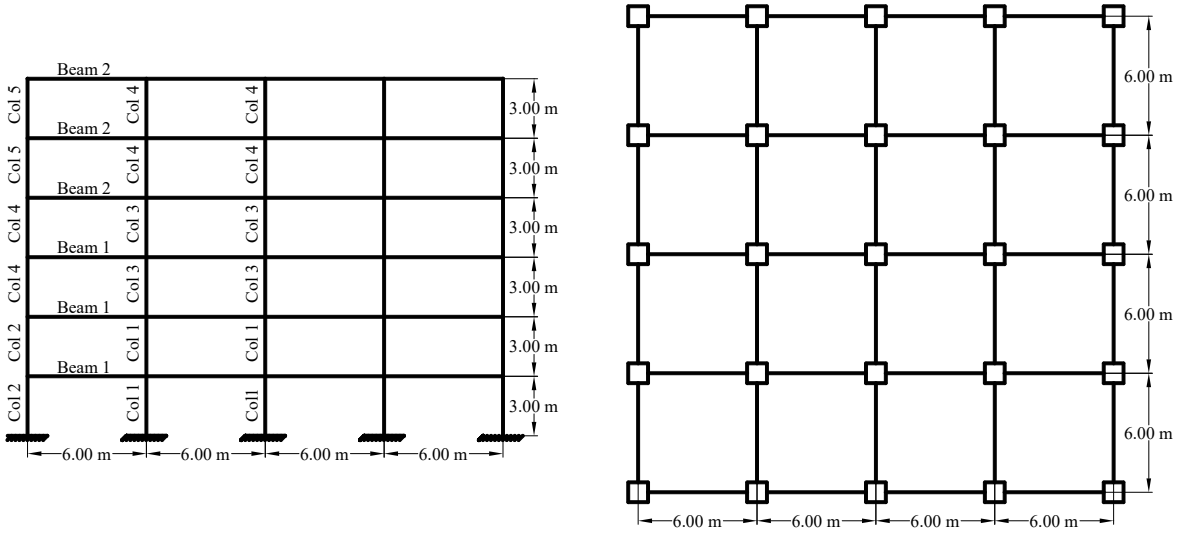

Fig. 6: Six-storey RC building Plan and Elevation (Youssef and Elfeki 2012)

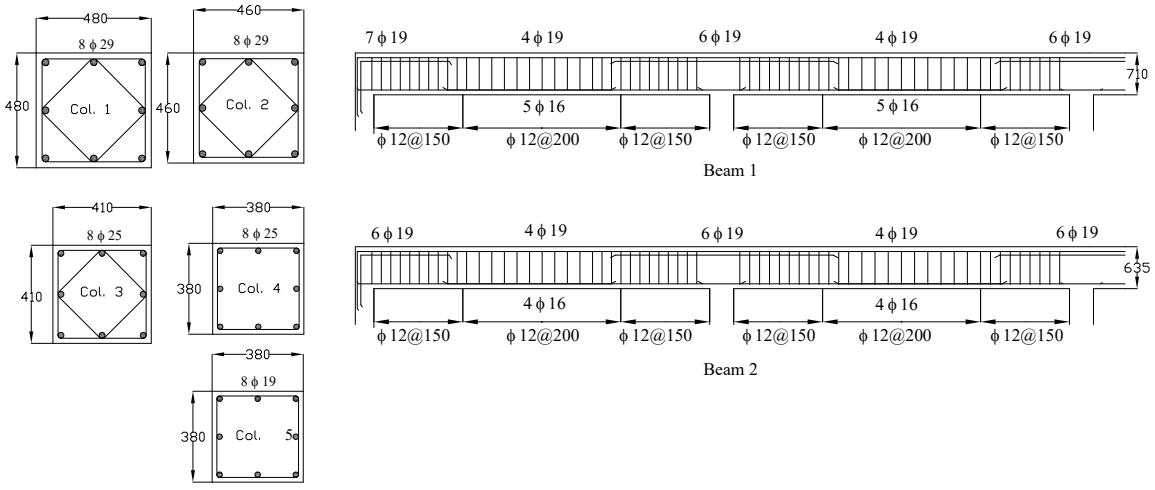

Fig. 7: Six-storey RC building cross-sections of beams and columns (Youssef and Elfeki 2012)

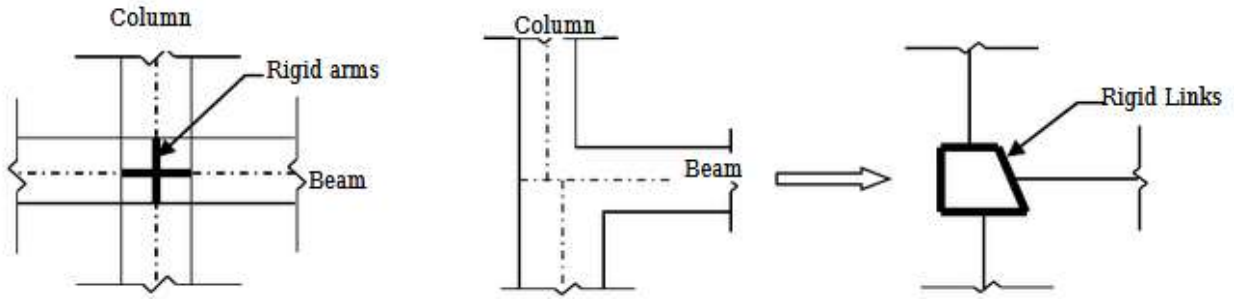

a) Interior beam-column joint b) Edge beam-column joint

Fig. 8: Modeling of beam column joints (Youssef and Elfeki 2012)

5 SMA RC FRAMES

Superleastic SMA bars are added to the steel RC frame to enhance its seismic performance. Two retrofitting schemes are proposed in this paper. The first retrofitting scheme is by retrofitting the BCJs of the first floor (Frame 2). The second retrofitting scheme is by retrofitting the BCJs of the first and fourth floors (Frame 3). The choice of these locations is based on the recommendations made by Youssef and Elfeki (2012). The internal steel reinforcement of the retrofitted BCJ is cut at the locations of the added SMA bars. This ensures that the behaviour of the retrofitted BCJs and frame is controlled by the superleastic SMA bars rather than the internal steel bars.

The amount of SMA reinforcement is chosen equal to the amount of internal steel reinforcement. The critical stress, critical strain, modulus of elasticity of the SMA bars are equal to 401 MPa, 0.007, 62.5 GPa respectively. The SMA bars are attached to the frame using external rigid steel angles and bolts. The retrofitted BCJs are modelled in the Seismostruct software using the simplified model.

6 LOCAL FAILURE AND COLLAPSE LIMITS

Local yielding of the RC element is assumed to happen when the reinforcement reaches its yielding strain. Yielding strain is defined as 0.002 for steel and as 0.007 for SMAs. Researchers have suggested different definitions for concrete failure. In this paper, crushing of concrete is assumed to occur either when the confined concrete reaches a value of 0.015 or when the stirrups reach their fracture strain, as proposed by Pauley and Priestley (1992). Collapse of the structure is assumed to occur when four of the columns located in the same storey reach their crushing strain (Youssef and Elfeki 2012).

7 DYNAMIC ANALYSES

7.1 Eigen Value Analysis

Eigen value analysis is performed for the steel RC frame by Youssef and Elfeki (2012). The fundamental period of vibration of the structure is found to be 0.501. The Eigen value analysis is repeated for the two retrofitted frames to investigate the effect of adding external SMA bars on the fundamental period of vibration. No or negligible effect is observed. **Fig. 9** shows the first four mode shapes for the three studied frames.

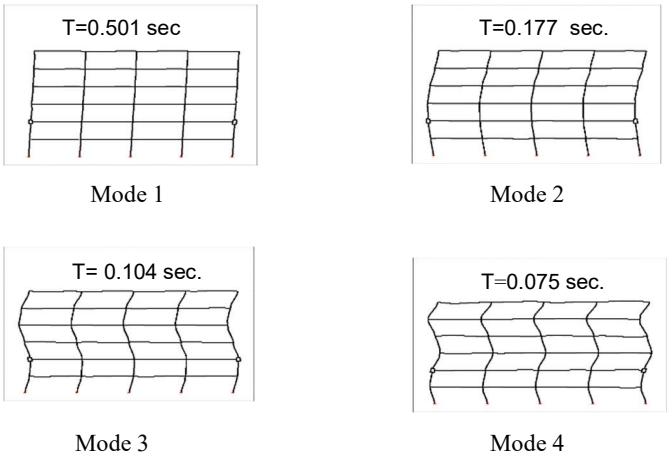

Fig. 9: First four mode shapes of Frames 1, 2, and 3

7.2 Selection of Ground Motion Records

The five ground motion records, used by Youssef and Elfeki (2012), are used in this study to perform the dynamic analysis of the frames. The ratio between the peak ground acceleration and the peak ground velocity (A/v) is used to classify the intensity of the used records. These records cover a wide range of ground motion frequencies. A summary of the record characteristics is given in **Table 1**.

Using a reliable method to scale the chosen records is critical when performing dynamic analysis. There are different methods available to scale the used ground motions such as scaling the Peak GroundAcceleration (PGA), scaling the peak ground velocity, and the 5% damped spectral acceleration at the structures first period (Youssef and Elfeki 2012, Shome and Cornell 1999, Vamvatsikos and Cornell 2002). The 5% damped spectral acceleration at the fundamental period

of the structure [Sa(T1,5%)] is used to scale the earthquake records in this study. **Fig. 10** shows the scaled earthquake records.

Table 1: Chosen earthquake records

Earthquake	Date	Ms Magnitude	Station	PGA (g)	A/v
Northridge USA	17/1/94	6.7	Arleta-Nordhoff	0.340	Inter.
Imperial Valley USA	15/10/79	6.9	El Centro Array #6 (E06)	0.439	Low
Loma Prieta USA	18/10/89	7.1	Capitola (CAP)	0.530	High
Whittier USA	1/10/87	5.7	Whittier Dam	0.316	High
San Fernando	9/2/71	6.6	Pacoima Dam	1.230	Inter.

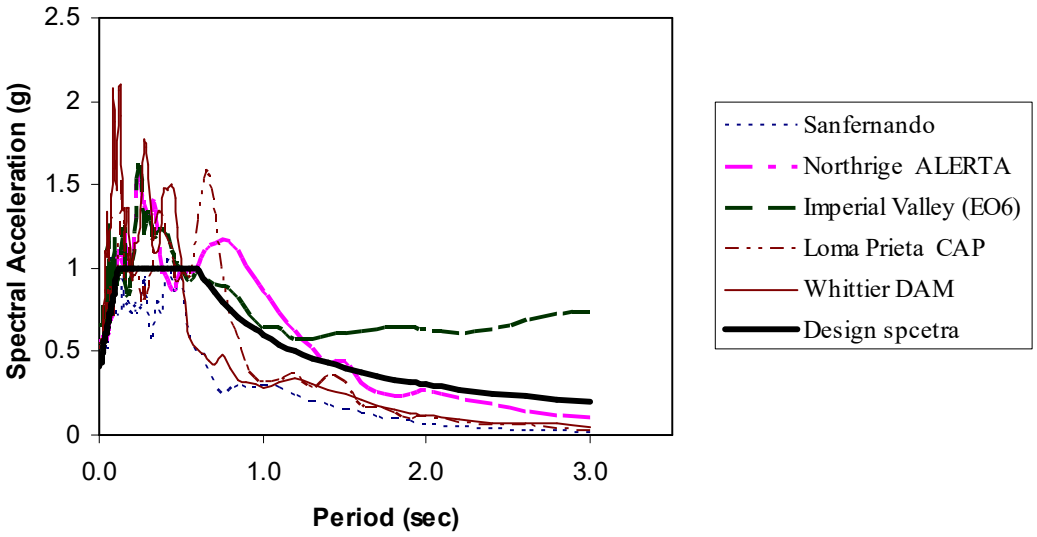

Fig. 10: Spectral acceleration diagrams

7.3 Incremental Dynamic Analysis (IDA)

Incremental Dynamic analysis is performed for the three frames to observe the effect of increasing the spectral acceleration on the behaviour of the frames. Results of the three frames are compared in terms of MID, MRID, MRDR, and RRDR. Performance of the three frames is then compared at the intensities causing collapse to Frame 1.

8 RESULTS AND DISCUSSIONS

Figs. 11 to **15** show the results obtained from the incremental dynamic analysis. **Fig. 11** illustrates the behaviour of the three frames when subjected to Imperial record. It is clear from the figure that the three frames experienced similar MID and MRDR at low values of Sa (T1, 5%). At high values of Sa (T1, 5%), Frame 1 experienced much higher MID and MRDR values. This shows the effect of the suggested retrofitting technique on limiting the MID and MRDR values. MRID and

RRDR behaviour is similar at low Sa (T1, 5%). However, at high values of Sa (T1, 5%), the suggested retrofitting technique showed much less values of residual drifts. Furthermore, Frame 3 (SMA at first floor only) showed lower residual drifts than Frame 2, which means better arrangement for the SMA bars.

Fig. 12 shows the response of the three frames to the Loma Prieta record. In this case, the three frames showed similar values of MID at all levels of Sa (T1, 5%). Frames 2 and 3 showed less values of MRDR close to failure. Frame 3 showed less residual drifts (MRID and RRDR) than frames 1 and 2. Frame 2 has MRID and RRDR values that are almost an average of the two other frames. **Fig. 13** shows the response of the three frames to the Northridge record. MID and MRDR values are similar for the three frames at all levels of Sa (T1, 5%). Residual drift (MRID and RRDR) values of frames 2 and 3 are much lower than frame 1 (steel RC frame). Frame 2 shows less MRID value at collapse, while Frame 3 shows less RRDR value at collapse.

Response of the three frames to the San Fernando record is shown in **Fig. 14**. The three frames have similar maximum and residual drift ratios at small levels of Sa (T1, 5%). At high levels of Sa (T1, 5%), Frames 1 and 3 show less MID values than frame 2. The difference increases as the Sa (T1, 5%) value increase. MRDR value is similar for the three frames at all levels of Sa (T1, 5%). For residual drifts (MRID and RRDR), the response of the three frames is similar at low values of Sa (T1, 5%) and at collapse. At intermediate values of Sa (T1, 5%), frame 1 shows higher residual drifts than frames 2 and 3.

Fig. 15 shows the response of the three frames to Whittier record. Similar response of the three frames is observed for MID and MRDR. At collapse, frame 1 shows higher MID value. Frames 2

and 3 show much less residual drifts at collapse. However, comparable values are observed at low levels of Sa (T1, 5%).

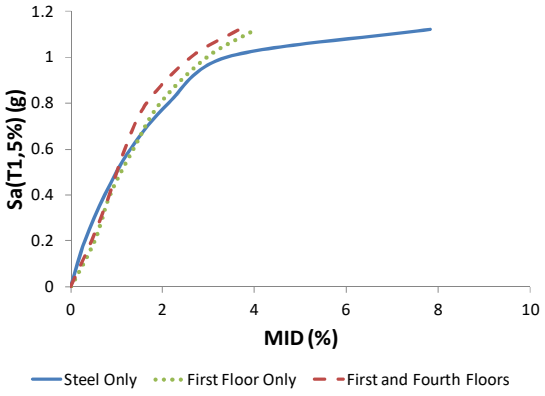

(a) Maximum Inter-Storey Drift

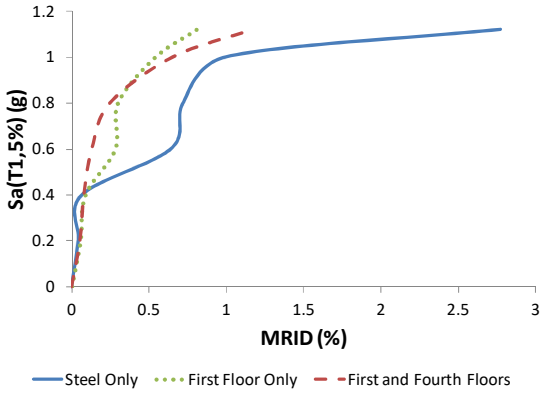

(b) Maximum Residual Inter-Storey Drift

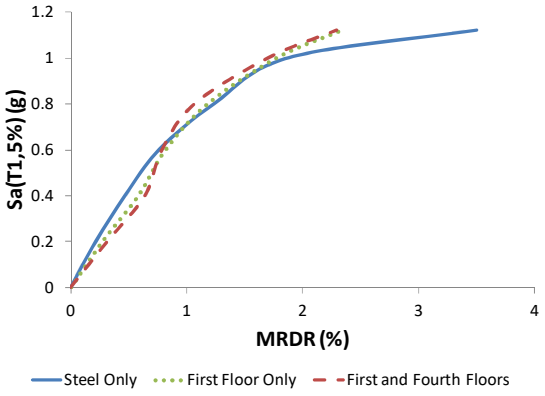

(c) Maximum Roof Drift Ratio

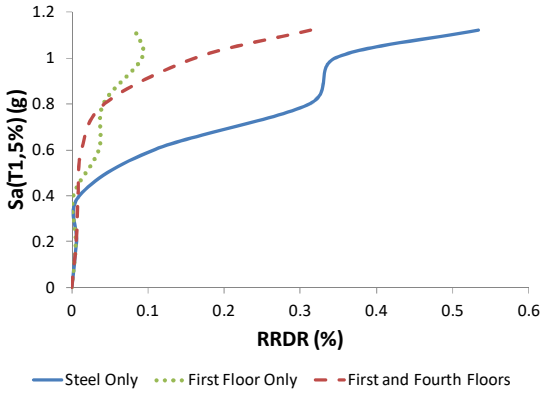

(d) Residual Roof Drift Ratio

Fig. 11: Incremental dynamic analysis of the three frames - Imperial Record

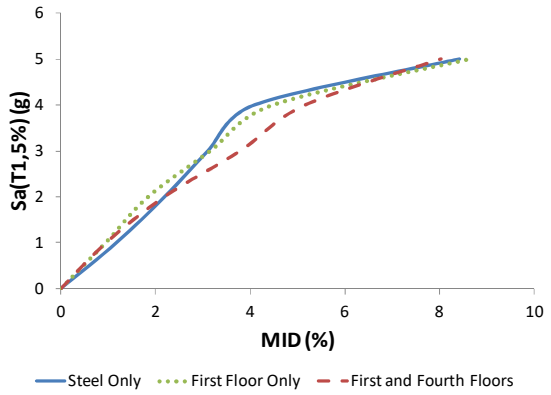

(a) Maximum Inter-Storey Drift

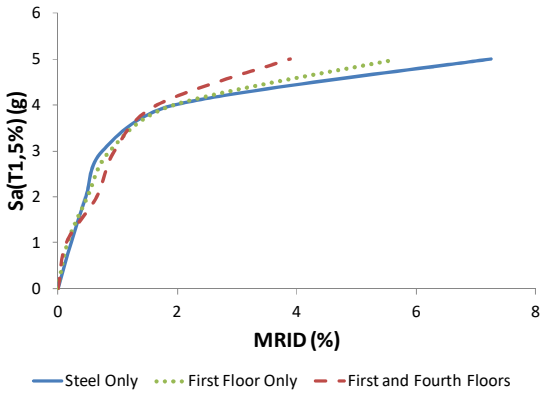

(b) Maximum Residual Inter-Storey Drift

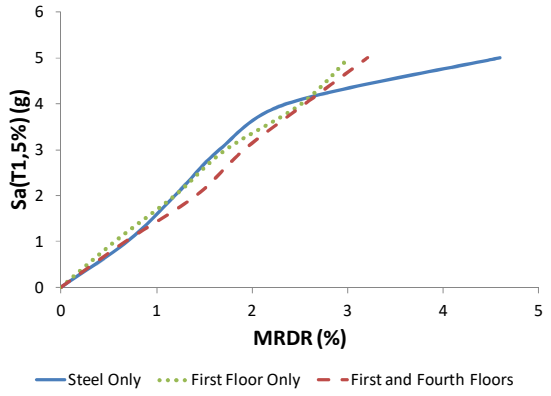

(c) Maximum Roof Drift Ratio

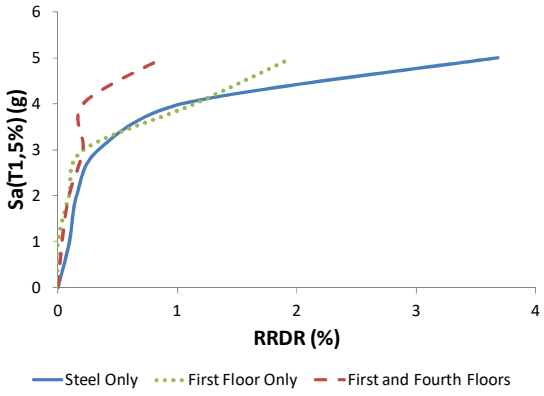

(d) Residual Roof Drift Ratio

Fig. 12: Incremental dynamic analysis of the three frames - Loma Prieta Record

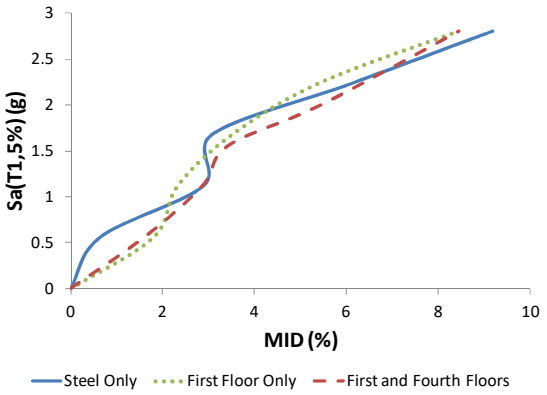

(a) Maximum Inter-Storey Drift

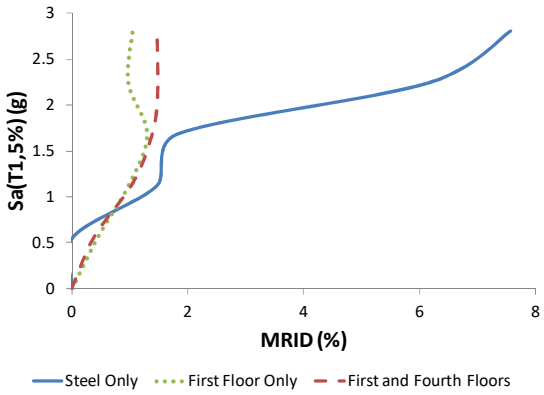

(b) Maximum Residual Inter-Storey Drift

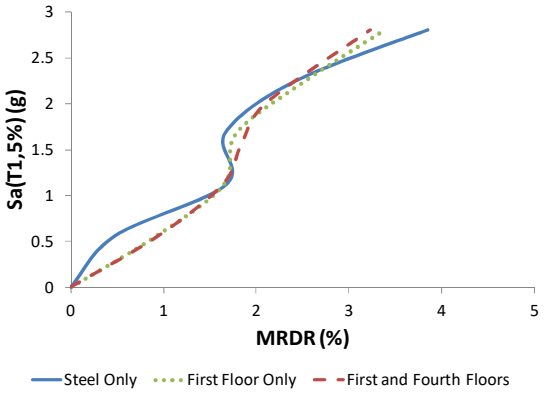

(c) Maximum Roof Drift Ratio

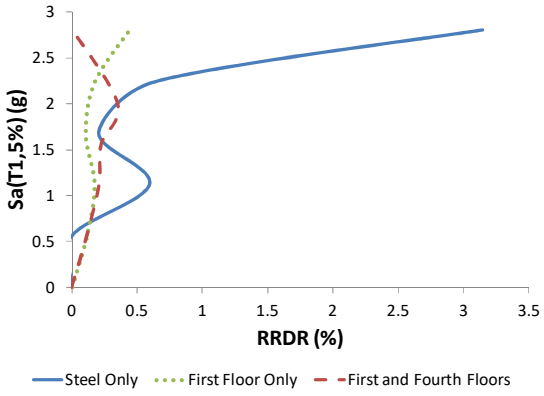

(d) Residual Roof Drift Ratio

Fig. 13: Incremental dynamic analysis of the three frames - Northridge Record

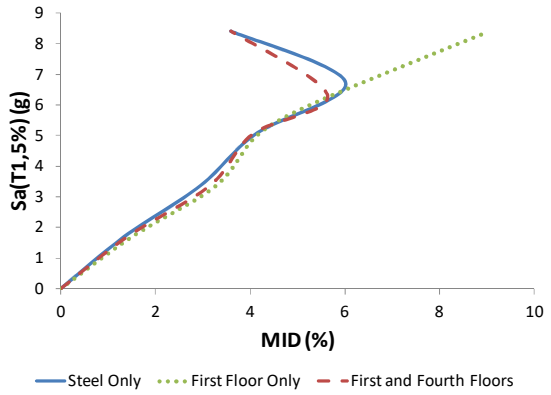

(a) Maximum Inter-Storey Drift

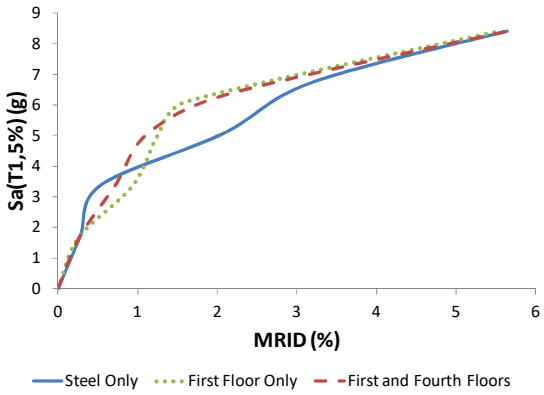

(b) Maximum Residual Inter-Storey Drift

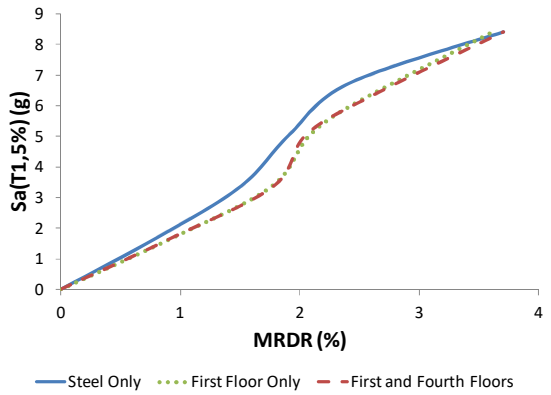

(c) Maximum Roof Drift Ratio

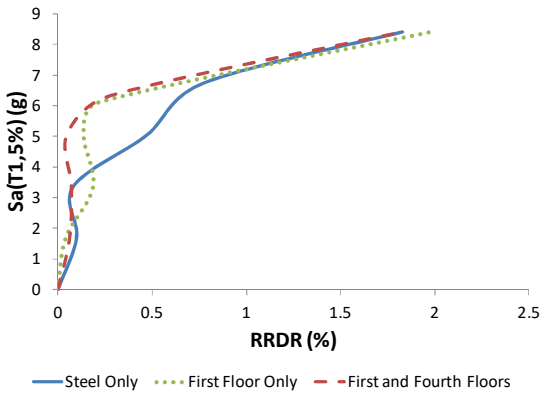

(d) Residual Roof Drift Ratio

Fig. 14: Incremental dynamic analysis of the three frames - San Fernando Record

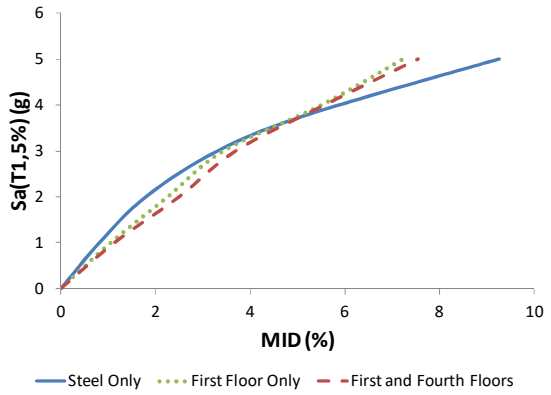

(a) Maximum Inter-Storey Drift

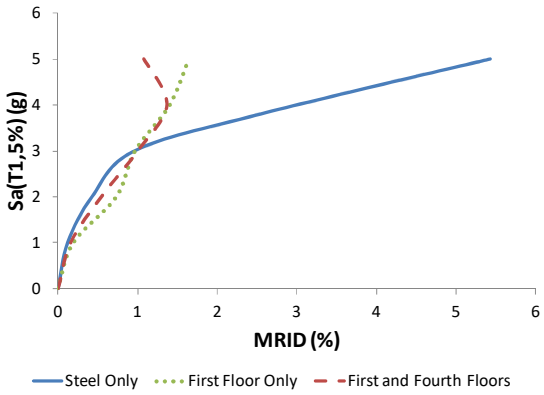

(b) Maximum Residual Inter-Storey Drift

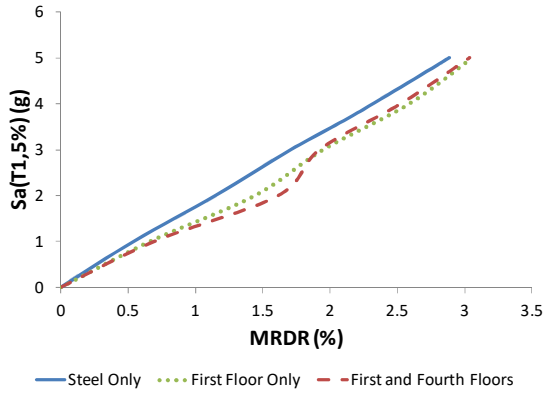

(c) Maximum Roof Drift Ratio

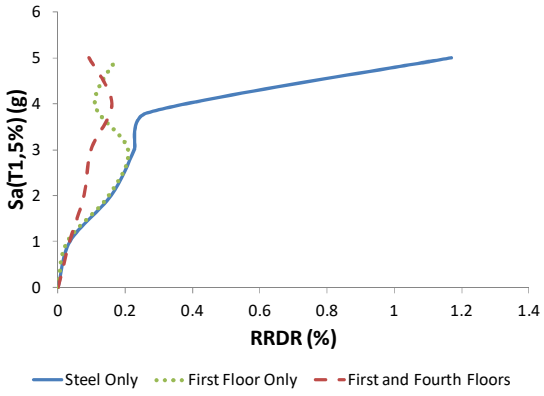

(d) Residual Roof Drift Ratio

Fig. 15: Incremental dynamic analysis of the three frames - Whittier Record

8.1 Damage Schemes

The damage schemes of the three frames at collapse when subjected to the five earthquake records are illustrated in **Figs. 16** to **20**. **Fig. 16** shows the damage scheme of the three frames when subjected to the Imperial Valley record. It is clear from the figure that Frame 1 (steel RC frame) reached its collapse limit due to the concrete crushing of the lower ends of the first storey columns. Frames 2 and 3 did not reach the collapse limit and can sustain higher loads as only three columns reached their crushing limit. No crushing is observed at higher storey columns. Most of the beams and columns of the three frames reached their yielding limit. First and second floor beams of Frame 1 sustained yielding at their mid-span. All beams of Frame 3 did not reach yielding at their mid-spans.

Fig. 17 shows the damage schemes of the three frames when subjected to the Loma Prieta earthquake record. Frame 1 reached its collapse limit by crushing of the lower four ends of the first storey columns. Frames 2 and 3 did not reach their collapse limit and can sustain higher loads. Most of the columns and beams reached their yielding limit. Most of the beams also reached their yielding limit at mid-span.

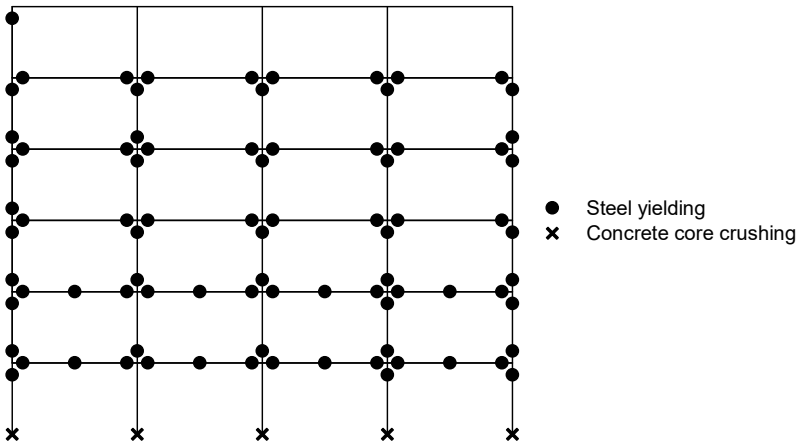

(a) Frame 1 (Steel Only)

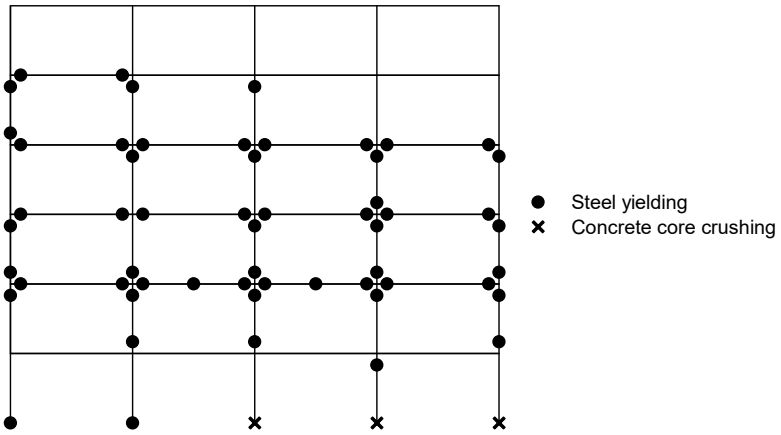

(b) Frame 2 (First Floor Only)

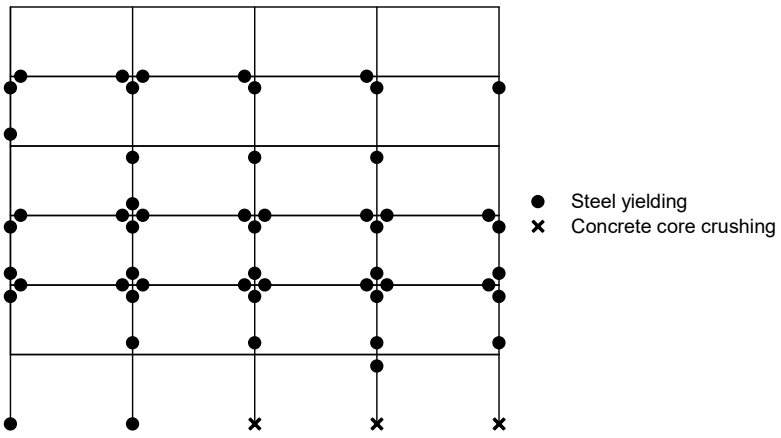

(c) Frame 3 (First and Fourth Floors)

Fig. 16: Damage scheme for different frames when subjected to Imperial earthquake record; (a) Frame 1 (Steel Only); (b) Frame 2 (First Floor Only); and (c) Frame 3 (First and Fourth Floors)

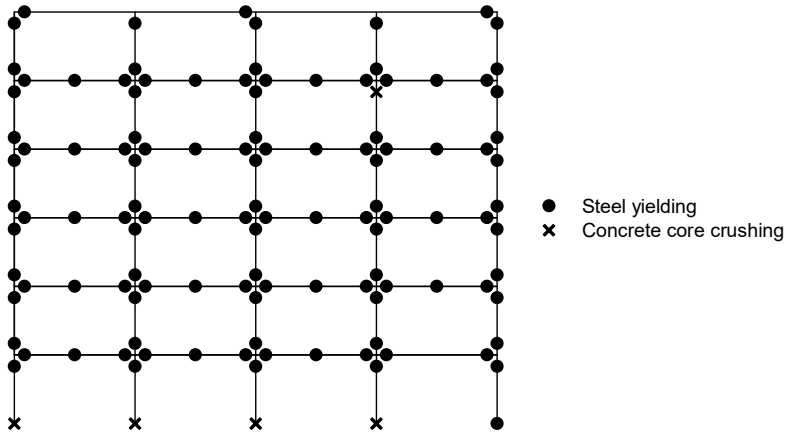

(a) Frame 1 (Steel Only)

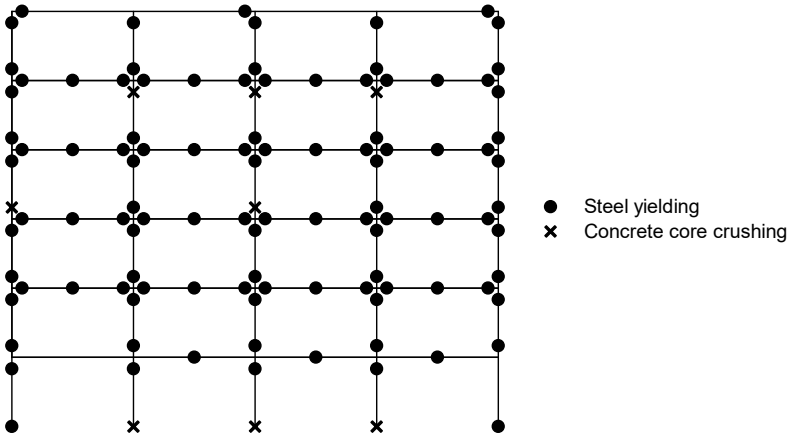

(b) Frame 2 (First Floor Only)

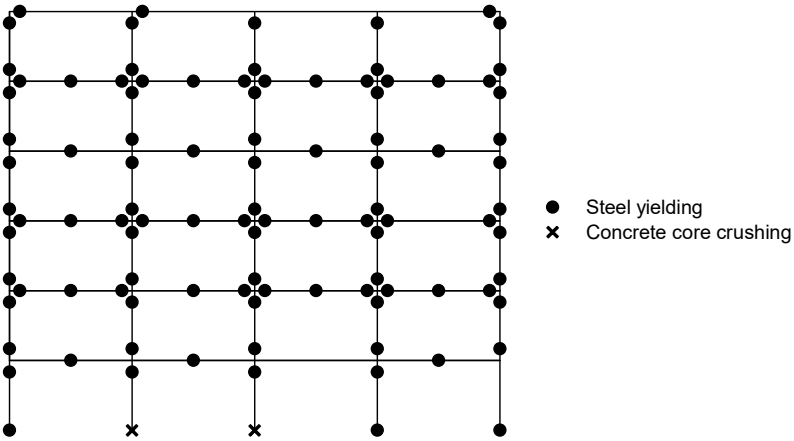

(c) Frame 3 (First and Fourth Floors)

Fig. 17: Damage scheme for different frames when subjected to Loma Prieta earthquake record; (a) Frame 1 (Steel Only); (b) Frame 2 (First Floor Only); and (c) Frame 3 (First and Fourth Floors)

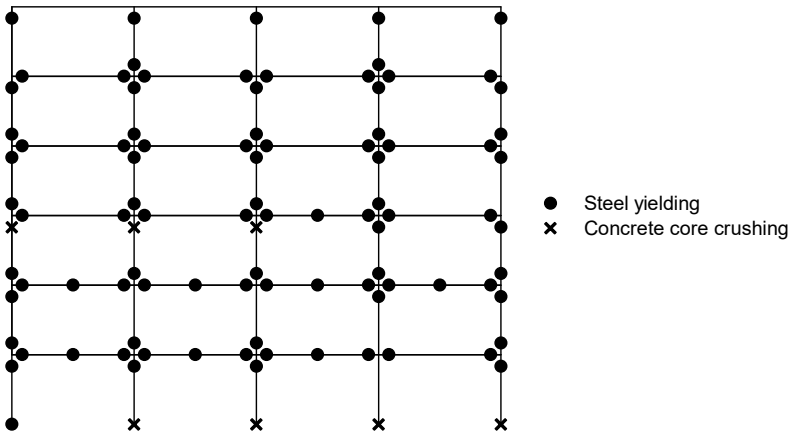

(a) Frame 1 (Steel Only)

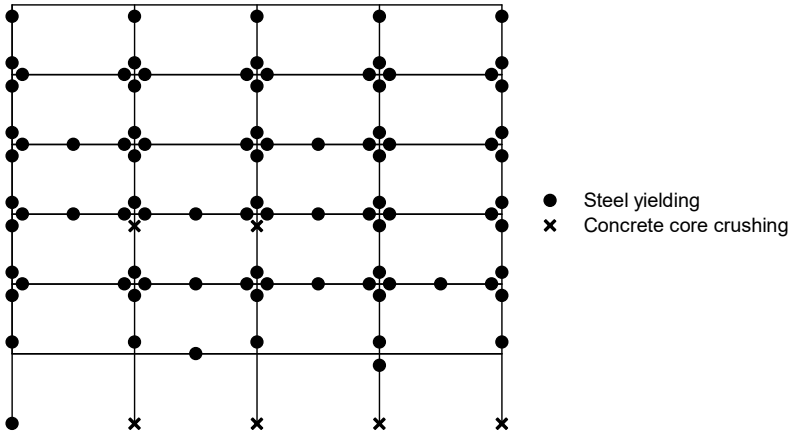

(b) Frame 2 (First Floor Only)

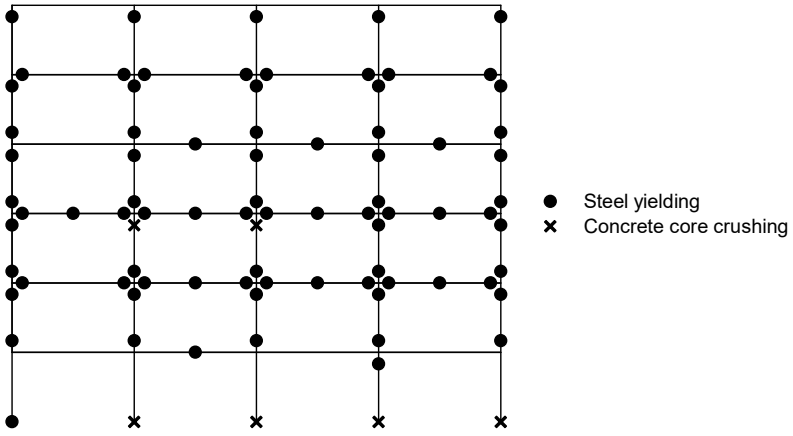

(c) Frame 3 (First and Fourth Floors)

Fig. 18: Damage scheme for different frames when subjected to Northridge earthquake record; (a) Frame 1 (Steel Only); (b) Frame 2 (First Floor Only); and (c) Frame 3 (First and Fourth Floors)

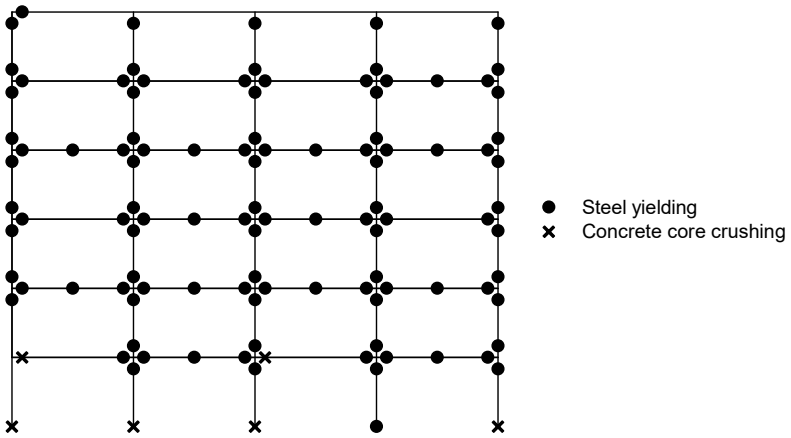

(a) Frame 1 (Steel Only)

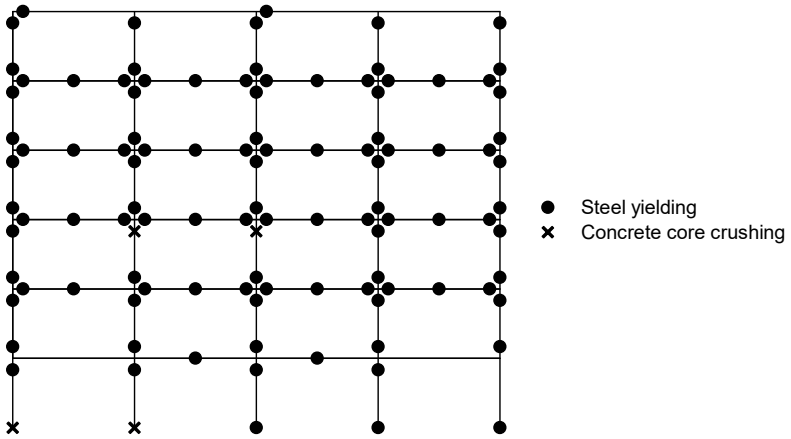

(b) Frame 2 (First Floor Only)

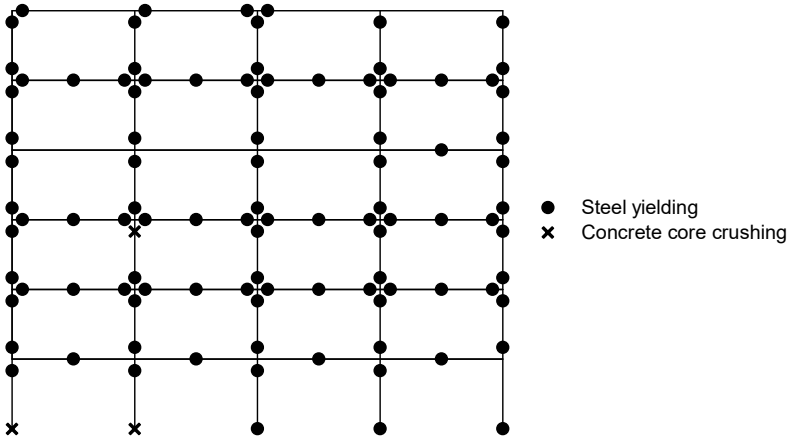

(c) Frame 3 (First and Fourth Floors)

Fig. 19: Damage scheme for different frames when subjected to San Fernando earthquake record; (a) Frame 1 (Steel Only); (b) Frame 2 (First Floor Only); and (c) Frame 3 (First and Fourth Floors)

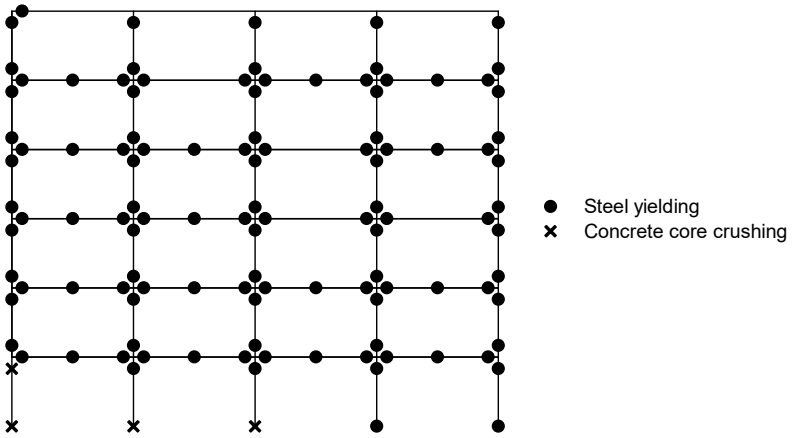

(a) Frame 1 (Steel Only)

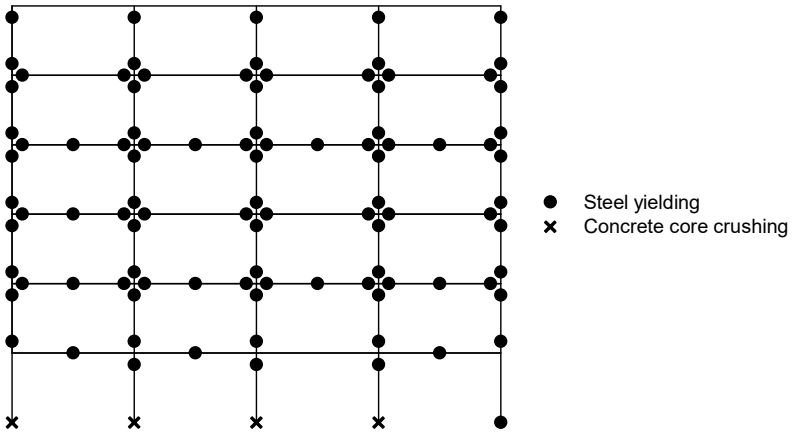

(b) Frame 2 (First Floor Only)

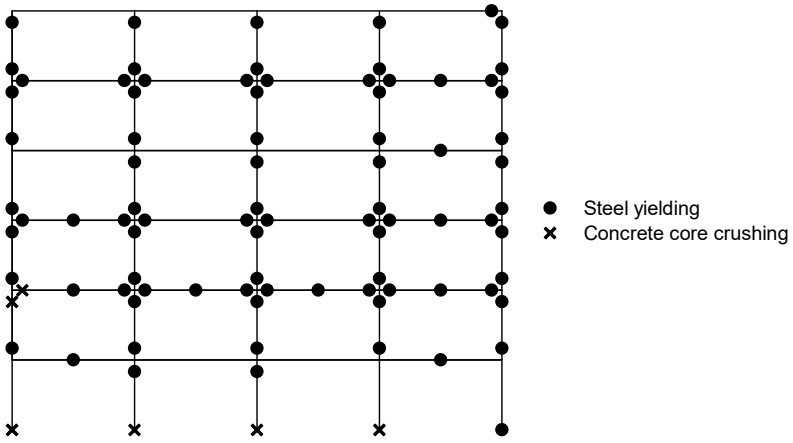

(c) Frame 3 (First and Fourth Floors)

Fig. 20: Damage scheme for different frames when subjected to Whittier earthquake record; (a) Frame 1 (Steel Only); (b) Frame 2 (First Floor Only); and (c) Frame 3 (First and Fourth Floors)

Damage schemes of the three frames when subjected to Northridge earthquake are shown in **Fig. 18**. The three frames reached their collapse limit due to concrete crushing of first storey columns. Three columns of the third storey of Frame 1 reached their crushing limits. Only two out of the three columns reached their crushing limits in Frames 2 and 3. Yielding of beams at their mid-spans is concentrated at the first two stories of Frame 1, and at the second, third and fourth stories of the other two frames.

The effect of the San Fernando earthquake on the three frames is shown in **Fig. 19**. Crushing occurred for first storey columns of Frame 1. In addition, two beams in the first storey reached their crushing limit. Frames 2 and 3 did not reach their collapse limit and resist higher levels of loads. Two columns in the third storey of Frame 2 reached their crushing limit, while only one column in the same location reached its crushing limit in Frame 3. Severe yielding of the beams and columns of the three frames can be observed. Mid-span yielding of the beams of the three frames is also observed.

The damage schemes of the three frames due to the Whittier earthquake are shown in **Fig. 20**. Collapse of the three frames occurred due to crushing of the first storey columns. Severe yielding of the beams and columns can be observed. One beam and one column in the second storey of Frame 3 reached their crushing limit. Mid-span yielding of the beams is more pronounced in case of Frames 1 and 2 than the case of Frame 3.

8.2 Maximum and Residual Drifts

MID, MRID, MRDR, and RRDR values at failure are used in this section to compare the behaviour of the three frames. Results of the three frames are given in **Table 2** and are illustrated in **Fig. 21**. The average MID for Frame 1 (steel RC frame) is found to be 8.40%. Frames 2 and 3 have lower average MID values 7.46 and 7.43, respectively. This shows the improvement in the frame behaviour by reducing the MID ratio.

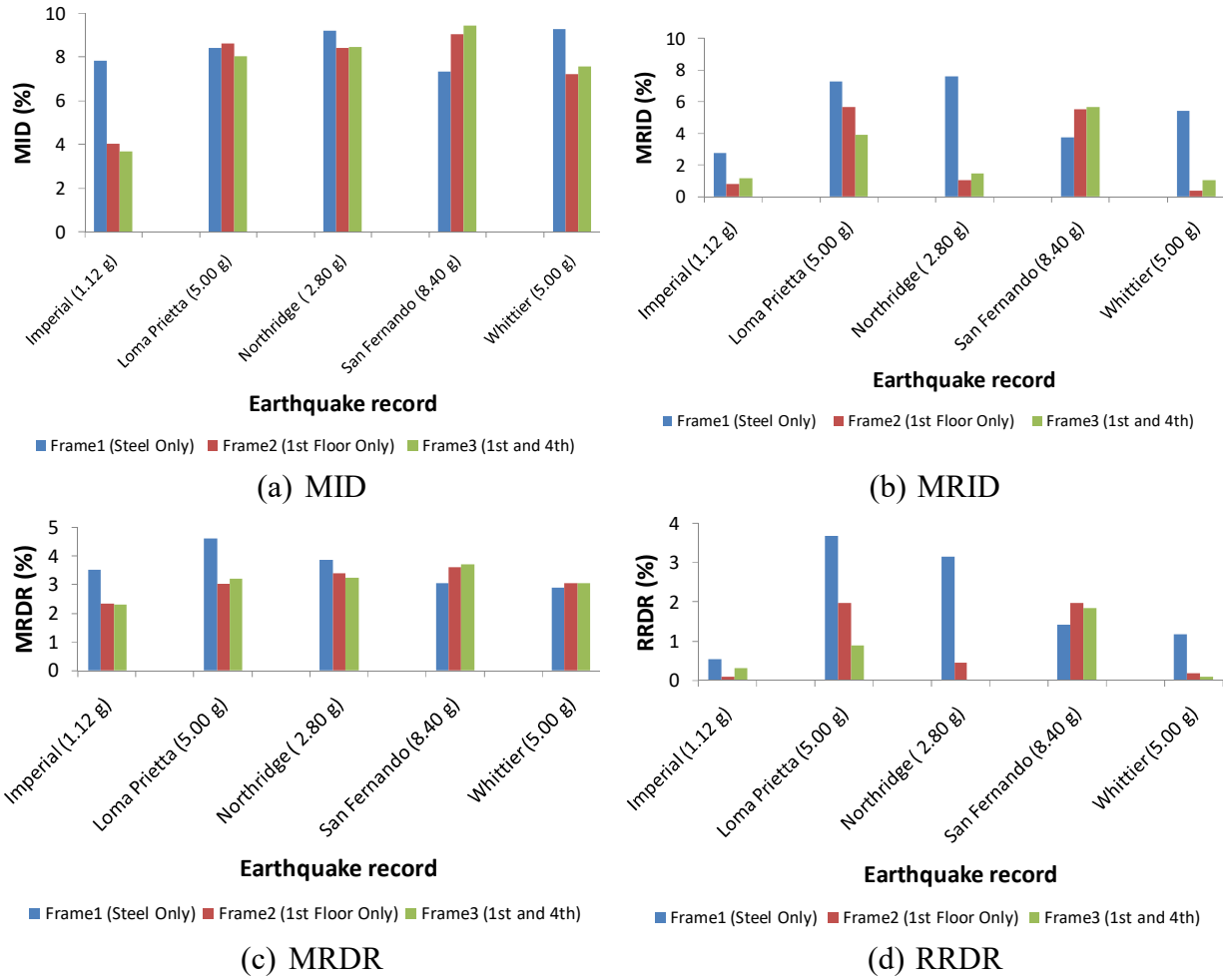

(a) MID (b) MRID

(c) MRDR (d) RRDR

Fig. 21: Maximum and residual drift ratios of the studied frames; (a) MID; (b) MRID; (c) MRDR; and (d) RRDR

Table 2: Comparison between the seismic performance of the three frames

Earthquake Record	Frame1 (Steel Only)				Frame2 (1st Floor Only)				Frame3 (1st and 4th)			
	MID	MRID	MRDR	RRDR	MID	MRID	MRDR	RRDR	MID	MRID	MRDR	RRDR
Imperial (1.12 g)	7.83	2.77	3.50	0.53	4.01	0.81	2.33	0.08	3.68	1.17	2.29	0.31
Loma Prietta (5.00 g)	8.41	7.25	4.60	3.68	8.60	5.66	3.01	1.96	8.02	3.89	3.21	0.88
Northridge (2.80 g)	9.18	7.56	3.85	3.15	8.43	1.05	3.37	0.44	8.45	1.47	3.23	0.01
San Fernando (8.40 g)	7.33	3.77	3.04	1.42	9.04	5.52	3.61	1.97	9.43	5.64	3.71	1.83
Whietter (5.00 g)	9.26	5.43	2.89	1.17	7.22	0.36	3.05	0.18	7.55	1.08	3.04	0.09
Average Value	8.40	5.36	3.57	1.99	7.46	2.68	3.08	0.93	7.43	2.65	3.10	0.62
Percent of Change	NA	NA	NA	NA	-11.20	-50.00	-13.96	-53.49	-11.63	-50.51	-13.40	-68.63

The improvement in the MRID value for frames 2 and 3 is found to be significant. The average MRID values of Frames 2 and 3 are 2.68% and 2.65% which are much lower (50.00% and 50.51%) of that of Frame 1 (5.36%). These values illustrate the significant improvement in the frame behaviour by adding the external SMA bars to the frame at the right locations.

The average MRDR is found to be 3.57% for Frame 1. This value is reduced by 13.96% for Frame 2 and by 13.40% for Frame 3. This confirms the reduction occurred in the MRID value of the frames. The RRDR significantly improved by adding the external SMA bars. The RRDR reduced from 1.99% for the steel RC frame to 0.93% and 0.62% for frames 2 and 3, respectively. These values correspond to percents of change equal to 53.49% and 68.63% for Frames 2 and 3, respectively.

These drift results in addition to the previously introduced damage schemes show that retrofitting an existing RC frame by adding external SMA bars at the right locations can lead to: (i) lower level of damage; (ii) small reduction in the MID and MRDR values (10%-15%); (iii) significant reduction (50%-70%) in the residual deformations represented by MRID and RRDR; and (iv) higher seismic capacity.

9 CONCLUSIONS

This paper investigates the applicability of using external SMA bars to enhance the seismic performance of steel RC frames. A six-storey steel RC frame building, located in a high seismic zone, is used as a reference for this study. Two potential retrofitting schemes using external SMA bars were assumed. The first frame is retrofitted at its first floor, while the second frame is

retrofitted at the first and fourth floors. Incremental dyanamic analysis is performed for the three frames to the collapse limit. After determining the collapse intensity for each record, the analysis is performed again for other two retrofitted frames. The two frames are retrofitted using the proposed retrofitting technique.

The performance of the three frames is compared based on the: (i) maximum tolerated earthquake intensity; (ii) level of damage; (iii) maximum drifts represented by MID and MRDR; and (iv) residual drifts represented by MRID and RRDR.

In terms of the damage schemes, the retrofitted frames showed lower level of damage at failure. They also tolerated higher earthquake intensities than the original steel RC frame. The suggested retrofitting technique reduced the maximum drifts of the frame by 10% to 15%, and the residual drifts by 50% to 70%. The two retroffited frames showed a similar behaviour. Thus, it is more economical to retrofit the steel RC frame using external SMA bars only at the first floor.

10 REFERENCES

ABAQUS F.E.A. (2018) ABAQUS Analysis user's manual. Dassault Systemes,Vélizy-Villacoublay, France, 2006.

ACI Committee 318 (2005) Building Code Requirements for Structural Concrete (ACI 318-05) and commentary (ACI 318R-05). American Concrete Institute, Farmington Hills MI, USA, 430 pp.

Alam MS, Nehdi M and Youssef MA (2009) Seismic Performance of Concrete Frame Structures Reinforced with Superelastic Shape Memory Alloys. Smart Structures and Systems 5(5): 565-585.

Alam MS, Youssef, MA, and Nehdi M (2007). Utilizing Shape Memory Alloys to Enhance the Performance and Safety of Civil Infrastructure: a Review. Canadian Journal of Civil Engineering, 34(9): 1075-1086.

Auricchio F, and Sacco E (1997) Superelastic shape-memory-alloy beam model. Journal of Intelligent Material Systems and Structures, 8(6): 489-501.

Engindeni M (2008) Repair and Strengthening of Pre-1970 Reinforced Concrete Corner Beam-Column Joints Using CFRP Composites. PhD dissertation, Georgia Institute of Technology, USA.

Hassan WM (2011) Analytical and Experimental Assessment of Seismic Vulnerability of Beam-Column Joints without Transverse Reinforcement in Concrete Buildings. PhD dissertation, University of California at Berkely, USA.

IBC (2006) International Building Code, International Code Council, ICC, Country Club Hills, IL, USA, 679 pp.

Janke L, Czaderski C, Motavalli M, and Ruth J (2005). Applications of Shape Memory Alloys in Civil Engineering Structures - Overview, Limits and New Ideas. Materials and Structures, 338(279): 578-592.

Paulay T, and Priestley MJN (1992) Seismic design of reinforced concrete and masonry buildings. John Wiley & Sons, New York, NY, USA.

SeismoSoft (2018) SeismoStruct - A computer program for static and dynamic nonlinear analysis of structures. Available from URL: http://www.seismosoft.com.

Youssef MA, and Elfeki MA (2012) Seismic Performance Concrete Frames Reinforced with Superelastic Shape Memory Alloys. Journal of Smart Structures and Systems, 9(4): 313-333.